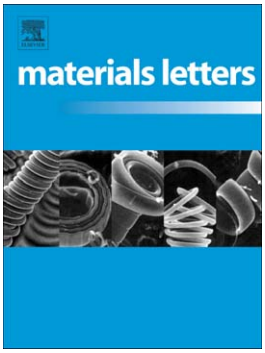

Synthesis and characterization of TiO_2-carbon nanocomposites with both micro- and mesopore size distributions

Xiaodong Wang, Guobin Zheng, Hideaki Sano, Zhijun Zhang, Yasuo Uchiyama

PII: S0167-577X(10)00579-3
DOI: doi: 10.1016/j.matlet.2010.07.037
Reference: MLBLUE 11390

To appear in: *Materials Letters*

Received date: 11 May 2010
Accepted date: 12 July 2010

Please cite this article as: Wang Xiaodong, Zheng Guobin, Sano Hideaki, Zhang Zhijun, Uchiyama Yasuo, Synthesis and characterization of TiO_2-carbon nanocomposites with both micro- and mesopore size distributions, *Materials Letters* (2010), doi: 10.1016/j.matlet.2010.07.037

Synthesis and characterization of TiO_2-carbon nanocomposites with both micro- and mesopore size distributions

Xiaodong Wang[1,2*], Guobin Zheng[2], Hideaki Sano[2], Zhijun Zhang[1] and Yasuo Uchiyama[2]

[1] Key Laboratory for Special Functional Materials, Henan University, Kaifeng 475004, China

[2] Department of Materials Science and Engineering, Faculty of Engineering,Nagasaki University, 1-14 Bunkyo-machi, Nagasaki 852-8521, Japan

Corresponding author, tel/fax: +86 378 3881358, Email address:donguser@henu.edu.cn

Abstract: TiO_2-carbon nanocomposites were synthesized by simply mixing a TiO_2 sol with a semi-cured resorcinol and formaldehyde gel, followed by drying and pyrolysis at 1000 ºC in an inert atmosphere. For comparison, the pure resorcinol and formaldehyde gel and the pure TiO_2 gol were also prepared, dried and pyrolysed in same conditions, respectively. The composites with a low TiO_2 content had the similar pore size distribution (PSD) and crystallographic structure to that of the blank sample (i.e., micropore size distribution), However the presence of high content TiO_2 in the composites effectively resulted in an increase in mesoporosity and a crystallographic structure of dominant rutile TiO_2 in the TiO_2-carbon nanocomposite.

Keywords: TiO_2, carbon, nano-composite, micro- and mesopore size distribution.

1. Introduction

The resorcinol and formaldehyde (RF) sol-gel method has been receiving considerable attention in the

literature during the past two decades or so[1-6]. By using this sol-gel method, several alkaline and transition metal ions, can be well dispersed in the RF gels and its carbonized derivatives during the synthesis process[1, 7-9]. The incorporation of metal ions in the RF gels or its carbonized derivatives leads to a hybrid material with potential applications as catalyst[7], supercapacitor[10], and lithium-ion battery anode[11].

TiO_2 has been widely used as a photocatalyst for photogeneration of hydrogen from water[12, 13], solar-energy conversion[14], and degradation of organic compounds[15], due to its high oxidative power, chemical stability, low cost, and non-toxicity. Much attention was also focused on its potential application in the electrode material of the lithium-ion battery[16-19]. Recently, the activated carbon-supported TiO_2 (TiO_2/AC) composites became to attract attention[20,21]. The TiO_2/AC composites have high photocatalytic activity in comparison with pure TiO_2 powder, because it could create many active sites for the photocatalytic degradation.

In this communication, we report on the first preparation of the TiO_2-carbon composites by mixing a TiO_2 sol with the semi-cured resorcinol and formaldehyde gel, followed by 85 ºC drying and pyrolysis in an inert atmosphere. It showed that a micro- and mesopore size distribution of the TiO_2-carbon nanocomposite can be adjusted by changing the TiO_2 content in the composite.

2. Experimental

The preparation procedure of TiO_2 sol was similar to that reported elsewhere[22]. The synthesis procedure of the TiO_2-carbon nanocomposite was as follows. The RF polymers were synthesized by the polycondensation of resorcinol (R) and formaldehyde (F) using an initial R:F molar ratio of 1:2. Deionized water (W) was used as the diluent and the R:W molar ratio was 1:170. n-

Hexadecyltrimethylammonium bromide (CTAB) and Na_2CO_3 were used as the surfactant and the basic catalyst, respectively. The mixture was stirred for 10min, then heated to 85 ºC and maintained at 85 ºC under continuous stirring until the solution lost fluidity. The slurries were transferred into glass flasks and sealed. Then, they were placed in an oven at 85 ºC for 4 hours for the semi-cure process. Subsequently, the semi-cured samples were washed with a certain amount of anhydrous ethanol for 3 times. Fresh solvent was replaced every time after vacuum filtration. The washed samples were mixed with the TiO_2-sol ethanol solution with different contents of TiO_2. The mixtures were kept at room condition for 14 hours, and then were dried at 85 ºC in an oven for 6 hours. After the drying process, the glass beakers were removed from the oven and left to cool down to room temperature. Then, the dried samples were milled to powders. Finally, the composites were prepared by pyrolysis of the gel powders at 1000 ºC in N_2. The final TiO_2 contents of the composites were 6.4, 12.2, 17.7, 34.1, 50.0, 54.7%, respectively. The pure RF gel and the pure TiO_2 gol were also prepared, dried and pyrolysed in same conditions, respectively. The final products were named as blank sample 1 and blank sample 2, respectively. The surface morphology and particle size of the composites were investigated using field emission scanning electron microscope (FESEM) (JEOL JSM-7500 FAM, the accelerated voltage and current were 5.0 kV and 10μA, respectively) and transmission electron microscope (TEM) (JEOL JEM-2010, accelerated voltage: 200kV, current density: 20 pA/cm^2)X-ray diffraction analysis (XRD) (Cu-Kα, RINT 2200V) was performed to study the crystal structures, crystallite sizes, and phase formation of the composites. N_2 adsorption and desorption isotherms of the blank samples and TiO_2-carbon nanocomposite were obtained at 77K with an automatic adsorption apparatus (TriStar 3000). The BET specific surface area (SSA, S_{BET}) and total pore volume (V_{tot}) were calculated by using the Brunauer-Emmett-Teller equation and the single point method, respectively. The average pore diameter

(D) was estimated from the equation 4 V_{tot}/ S_{BET}. Micropore SSA (S_{mic}) was calculated by subtracting external SSA from BET SSA. The corresponding PSD were calculated with the desorption data based on the BJH method. The TiO_2 content was calculated by the loss on ignition of composites at 1000 ºC in air.

3. Results and discussion

PSD curves of the blank sample 1, the blank sample 2 and the TiO_2-carbon nanocomposites are shown in **Figure 1a**. It follows that the blank sample 1 mainly contains micropores and has a high BET surface area (542.58$m^2 \cdot g^{-1}$). When TiO_2 content is < 34.1 wt.%, the composites have the similar PSD with that of the blank sample 1, namely, the micropore size distribution. However, the composites with lower TiO_2 content have the lower BET surface area than those of the blank sample 1. For TiO_2 content ≥ 34.1 %, **Figure 1a** showed that the mesopore peak appeared. It is noteworthy that the ratio of the intensity of the mesopore (3~4nm) peak to that of the micropore peak increased obviously with the increase of the TiO_2 contents of the composites, indicating that the mesoporosity of the composites with a high TiO_2 content was much more developed than those of the composite with a low or zero TiO_2 content. Despite this, the BET surface areas of the composite with a high TiO_2 content also deteriorated. For the blank sample 2, it has a very low BET surface area (2.76 $m^2 \cdot g^{-1}$) and no obvious micropore peaks or mesopore peaks can be observed.

The XRD patterns of the blank sample 1, the blank sample 2 and the TiO_2-carbon nanocomposite are shown in **Figure 1b**. It is noticeable that when TiO_2 content < 34.1%, the composites have the similar structure with that of the blank sample 1. i.e., two broad peaks associated with the (002) and (10*l*) reflections from carbon are dominant, except that the weak rutile (110) peak and anatase (110) peak for the 12.2% TiO_2 content, and a weak rutile (110) peak for the 17.5 % TiO_2 content were observed,

respectively. According to Bragg equation, interplanar space (d_{002}) calculated to the blank sample 1 are about 0.42nm, > 0.35nm, indicating a considerably low-graphitization-degree carbon or amorphous carbon[23, 24]. When TiO_2 content ≥ 34.1%, sharp rutile peaks were dominant, and weak anatase (110) peaks could be still observed. C (002) peak almost disappeared and only weak (10*l*) peak (2θ=43.1º) probably attributed to graphitic carbon remained. For the blank sample 2, the 43.1º peak disappeared and only the narrower rutile TiO_2 peaks could be observed.

Figure 2 shows the morphologies of TiO_2-carbon nanocomposite containing 50 % of TiO_2. From the TEM (**Figure 2a**), we can observe that a lot of TiO_2 particles were well dispersed on the surfaces of the carbon nano-spheres. The diameters of TiO_2 particle and carbon sphere are 10~20nm and ca. 90 nm, respectively. The typical HRTEM image of the composite is shown in **Figure 2b**. The d-spacing of 0.295 nm corresponds to the (001) plane of rutile. The XRD pattern of composite containing 50.0 % of TiO_2 (**Figure 1b**) showed narrow diffraction peaks, which correspond to the rutile TiO_2. By Scherre's formula, the diameter of TiO_2 particle was calculated to be 19nm, which is consistent with the result of HRTEM. From the TEM image (Figure 3) of the blank sample 2, the rutile TiO_2 particles aggregated and the diameter of the particles is ca. 200nm, which is larger than those of the composite containing 50% of TiO_2. This indicates that the carbon can inhibit the growth and aggregation of TiO_2 particles.

4. Conclusions

In summary, we report a novel method to prepare TiO_2-carbon composites. The composites with a low TiO_2 content had the similar pore size distribution (PSD) and crystallographic structure to that of the carbon derived from the RF polymer (i.e., micropore size distribution), but the presence of high content TiO_2 in the composites effectively resulted in an increase in mesoporosity and a presence of a

crystallographic structure of dominant rutile TiO_2 in the TiO_2-carbon nanocomposites. The TiO_2-carbon nanocomposites with both mesopore and micropore distribution probably makes it suitable for an application as a material for electrodes of the secondary battery or an efficient photocatalyst.

Acknowledgments

The authors acknowledge the financial support by Japan's Official Development Assistance (ODA) to China.

References

[1] Pekala RW. US Patent 4873218.

[2] Pekala RW. J Mater Sci 1989; 24: 3221-3227.

[3] Tamon H, Ishizaka H, Mikami M., Okazaki M. Carbon1997; 35: 791-796.

[4] Yamamoto T, Sugimoto T, Suzuki T, Mukai SR, Tamon H. Carbon 2002; 40: 1345-1351.

[5] Jung HH, Hwang SW, Hyun SH, Lee KH, Kim GT. Desalination 2007; 216: 377-385.

[6] Elsayed MA, Hall PJ, Heslop MJ. Adsorption 2007; 13: 299-306.

[7] Rojas-Cervanes ML, Alonso L, Díaz-Terán J, López-Peinado AJ, Martín-Aranda RM, Gómez-Serrano V. Carbon 2004; 42: 1575-1582.

[8] Aguado-Serrano J, Rojas-Cervantes ML, Martín-Aranda RM, López-Peinado AJ, Gómez-Serrano V. App Surf Sci 2006; 252: 6075-6079.

[9] Aguado-Serrano J, Rojas-Cervantes ML, López-Peinado AJ, Gómez-Serrano V. Micropor Mesopor Mat 2004; 74: 111-119.

[10] Hwang SW, Hyun SH. J Power Sources 2007; 172: 451-459.

[11] Han S, Jang B, Kim T, M. Oh S, Hyeon T. Adv Funt Mater 2005; 15: 1845-1850.

[12] Fujishima A, Honda K. Nature 1972; 238: 37-39;

[13] Khan SUM, Al-Shahry M, Ingler Jr WB. Science 2002; 297: 2243-2245.

[14] O'Regan B, Grätzel M. Nature 1991; 353: 737-740.

[15] Mahmoodi NM, Limaee NY, Arami M, Borhany S, Mohammad-Taheri M. J. Photochem Photobiol A: Chem 2007; 189: 1-6.

[16] Wagemaker M,Kentgens APM, Mulder FM. Nature 2002; 418: 397-399.

[17] Liu Y, Lee JY, Hong L. J Appl Polym Sci 2003; 89: 2815-2822.

[18] Subramanian V, Karki A, Gnanasekar KI, Fannie Posey Eddy, B. Rambabu J Power Sources 2006; 159: 186-192.

[19] Qiao H, Xiao LF, Zhang LZ. Electrochem Commun 2008; 10: 616-620.

[20] Li YJ, Ma MY, Wang XH, Wang XH. J Environ Sci 2008; 20: 1527-1533.

[21] He Z, Yang SG, Ju YM, Sun C. J Environ Sci 2009; 21: 268-272.

[22] Zhang M, Feng CX, Jin ZS, Cheng G, Du ZL, Dang HX, Chinese J Catal 2005; 26: 1-6.

[23] Cuesta A, Dhamelincourt P, Laureyns J, Martinez-Alonso A, Tascón JMD. J Mater Chem 1998; 8: 2875-2879.

[24] Filho C de A, Zarbin AJG. Carbon 2006; 44: 2869-2876.

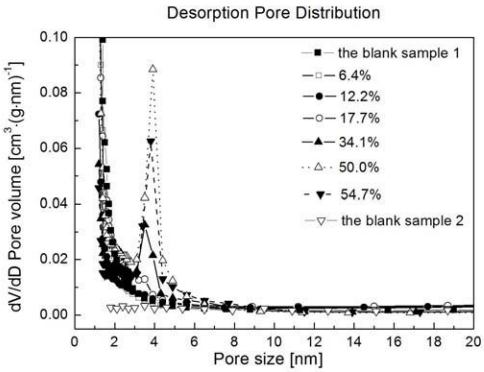

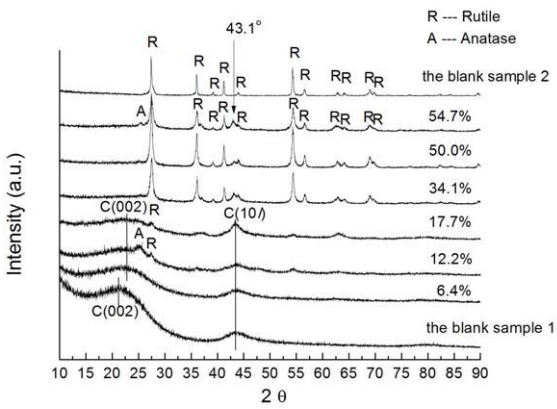

Figure 1a Figure 1b

Figure1 PSDs (a) and XRD patterns (b) for the blank samples and the TiO_2-carbon nanocomposites with different real TiO_2 contents

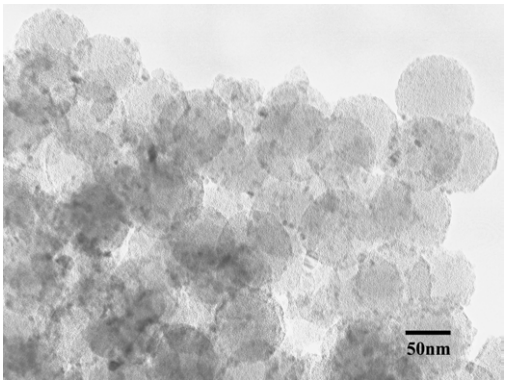

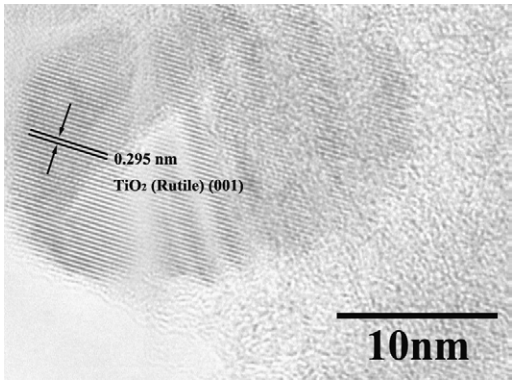

Figure 2a Figure 2b

Figure 2 the morphologies of TiO_2-carbon nanocomposite containing 50 % of TiO_2

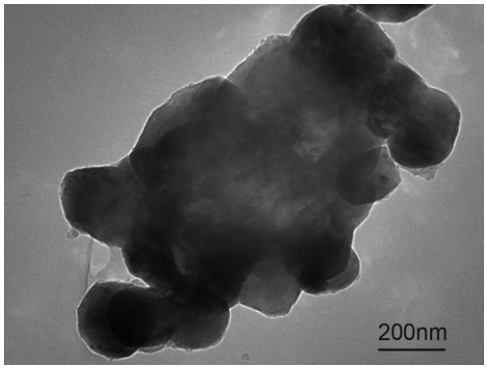

Figure 3 TEM image of the blank sample 2